applied sciences

MDPI

Article

An Automated Parametric Surface Patch-Based Construction Method for Smooth Lattice Structures with Irregular Topologies

Luisa Fleig * and Klaus Hoschke

Fraunhofer Institute for High-Speed Dynamics, Ernst-Mach-Institut, EMI, 79104 Freiburg, Germany; klaus.hoschke@emi.fraunhofer.de

* Correspondence: luisa.fleig@emi.fraunhofer.de

Abstract: Additive manufacturing enables the realization of complex component designs that cannot be achieved with conventional processes, such as the integration of cellular structures, such as lattice structures, for weight reduction. To include lattice structures in component designs, an automated algorithm compatible with conventional CAD that is able to handle various lattice topologies as well as variable local shape parameters such as strut radii is required. Smooth node transitions are desired due to their advantages in terms of reduced stress concentrations and improved fatigue performance. The surface patch-based algorithm developed in this work is able to solidify given lattice frames to smooth lattice structures without manual construction steps. The algorithm requires only a few seconds of sketching time for each node and favours parallelisation. Automated special-case workarounds as well as fallback mechanisms are considered for non-standard inputs. The algorithm is demonstrated on irregular lattice topologies and applied for the construction of a lattice infill of an aircraft component that was additively manufactured.

Keywords: smooth lattice structure; parametric construction; wireframe solidification; filleted node; surface patch; irregular lattice topology

Citation: Fleig, L.; Hoschke, K. An Automated Parametric Surface Patch-Based Construction Method for Smooth Lattice Structures with Irregular Topologies. *Appl. Sci.* **2023**, *13*, 11223. https://doi.org/10.3390/app132011223

Academic Editors: Loucas Papadakis, Ioannis Ntintakis and Stavroulakis Georgios

Received: 7 September 2023
Revised: 7 October 2023
Accepted: 10 October 2023
Published: 12 October 2023

1. Introduction

Lattice structures are cellular structures consisting of interconnected struts [1]. Each lattice structure is based on a lattice frame, also denoted as a wireframe, which describes with nodes and edges the inherent topological skeleton. The latter can either be irregular or consists of periodically repeated unit cells. Besides the interconnections and coordinates described by the lattice frame, the cross-section shapes and radii of the struts are local shape parameters of lattice structures.

Lattice structures find use in various disciplines, often in connection with additive manufacturing, reaching from architecture and mechanical engineering to healthcare [2,3]. Applications include medical implants [4], heat sinks [5], and crash boxes [6], exploiting the porous structure of lattices for the ingrowth of bones, the more efficient heat dissipation due to very high surface-to-volume ratio, and the high specific energy absorption capability by allowing for controlled deformation with reduced peak loads and good load uniformity. Lattice structures are particularly suitable for lightweight designs due to their high stiffness–weight ratio [3] and therefore find use in components that are designed for aeronautics and space applications [7,8]. In [8], additively manufactured lattice structures are used as cellular infills in areas where the topology optimisation of the discussed component recommends material densities between void and solid. Even entire components consisting of lattice structures are derived in [9] from topology optimisation results. To solidify the proposed (often irregular) wireframes in CAD software, an automated algorithm is required. Many commercial CAD software tools rely on spline-based surface patches that are exactly parametrisable by their control points. To integrate the design of lattice structure infills in the design process of the surrounding component, a method based on surface patches is

favourable. Having a component design based on splines is also advantageous for additive manufacturing, because it enables local manipulations, i.e., to remove large overhangings and to create support-free printable structures.

Besides the wireframe topology, smooth node transitions, also called filleted nodes, are an important aspect of lattice structure design as they can improve the structural response to loadings by reducing local stress concentrations and increasing the stiffness [10,11]. Additionally, the realisability of strut radii gradients, useful for further tailoring the lattice structure to an intended use, is improved in smooth lattice structures, according to [12].

Several methods to construct smooth lattice structures can be found in the literature, including polygon mesh methods [11,13,14], iso-surface methods [10,15,16], and surface patch methods [12,17]. Their key properties are summarised in Table 1. Their commonality is the construction of the lattice structures surface instead of a solid object. In [11,13,14], lattice structures are described with polygon meshes. Starting with simple mesh models, subdivision schemes are applied to refine the mesh, leading to smooth strut intersections. The main disadvantage of polygon mesh-based approaches is the inexact parametrisability of local shape parameters such as strut radii, as discussed in [11]. In [10,15,16], the definition of lattice structures with iso-surfaces is based on surface equations that map the three-dimensional space to the set of real numbers. The lattice structure is defined by the set of points that is mapped to values smaller or equal to zero. Thus, the zero-value iso-surface describes the lattice structures' surface. Thereby, the lattice structures' smoothness is inherited from the surface equations. Construction methods assembling the lattice structures' surface with surface patches are presented in [12,17]. Boundary conditions ensure smooth transition between patches. However, the available algorithms for this method either require manual construction steps or are restricted to periodic topologies.

The complex task of smoothly solidifying a wide range of different node topologies in lattice frames with irregular topology is either solved manually [17] or with convex hull algorithms [11,13,14].

Regarding the possibility to respect different local shape parameters such as strut radii gradients within the lattice structure, the reviewed methods face different limitations. Polygon mesh-based approaches allow for different strut radii in the definition of the initial mesh model. According to [11], the application of subdivision schemes during the smoothing process leads to deformations in these initial radii and cross-section shapes. Therefore, parameters have to be selected carefully or manually and extensive post-processing is required. Furthermore, an exact parametrisation is impossible. In [10], an iso-surface construction method with varying strut radii is discussed that allows for radius gradients along vectors. Consequently, the radii are not separately parametrisable for each strut. In [16], the iso-surface construction method is combined with threshold distribution fields that allow for the local exact radii parametrisations of individual struts. However, the wireframe topology supported by this method is unit cell-based. Surface patch methods offer the possibility of exact strut radii parametrisation, as it is shown in [12]. Nevertheless, the algorithm developed in [12] is also restricted to periodic lattice structures with repeated unit cells. So far, the only known surface patch-based approach for constructing irregular lattices with smooth surfaces requires manual construction steps [17]. Therefore, the objective of this work was to develop an automated surface patch-based algorithm without manual construction steps that is able to construct smooth lattice structures based on given lattice frames and strut radii for as general cases as possible. The method expanded on in this work has been applied by the authors for constructing a planar lattice as an infill for a lightweight structure in [8]. The algorithm is implemented as a macro in the commercial software CATIA V5-R2019; however, it can be used in any computer-aided design software that supports the three basic surface construction methods discussed in Section 2.

Table 1. Comparison of polygon mesh methods (PMMs), iso-surface methods (ISMs), and surface patch methods (SPMs) regarding the features' automation, irregular topology, and exact parametrisability.

Method	Automatisation	Irregular Topology	Exact Parametrisability
PMM	✓	✓	✗
ISM	✓	✗	✓
SPM	✗	✓	✓

2. Surface Construction Methods

The lattice structure is to be constructed as a free-form surface [18], meaning that it does not belong to a more easily recognised class of surfaces like cylinders or spheres due to the desired smoothness and irregular topology. According to [18], free-form surfaces are here constructed using a segmentation into local parametrisations of the surface, also denoted as *surface patches* [19]. To ensure smoothness, G^1-continuity is imposed between neighbouring patches. Two surfaces having a common boundary curve are called *geometric continuous*, written G^1*-continuous*, if they have a continuously varying tangent plane along that boundary curve [20]. If two surfaces have a common boundary curve but different tangent planes along that curve, the transition is called G^0*-continuous*. Within the proposed algorithm, surface patch construction methods for the following three base cases are required:

1. Given two curves $b, c : [0,1] \to \mathbb{R}^3$, the *ruled surface* $r : [0,1] \times [0,1] \to \mathbb{R}^3$ defined by $r(s,t) := s \cdot b(t) + (1-s) \cdot c(t)$ linearly interpolates b and c [20]. Figure 1a shows an example for the latter. In the developed algorithm, they are used for the definition of cross-boundary tangent conditions to ensure G^1-continuity of further constructed surface patches.
2. If the ruled surface matches additional cross-boundary tangent conditions along b and c, it is denoted as G^1*-continuous ruled surface*. An example is illustrated in Figure 1b. A method to impose geometric continuity on ruled surfaces can be found in [21]. This type of surface patch is used for the construction of struts and for smooth transitions between strut ends that converge to the same node.
3. Given a set of N boundary curves $c_1(t), \ldots, c_N(t)$ forming a loop, a surface patch filling the region inside the loop and meeting cross-boundary tangent conditions is denoted as G^1*-continuous N-patch*. In Figure 1c, a G^1-continuous 3-patch is sketched. Algorithms to construct this type of surface patch can be found in [22–24]. They are used in the lattice construction algorithm to fill regions between strut ends and their smooth transitions.

Based on the wireframe topology and local shape parameters of the lattice structure, a set of ruled surfaces is constructed to define cross-boundary tangent conditions for the subsequently defined G^1-continuous ruled surface patches that form the struts and that define the node transition. Lastly, G^1-continuous 6-patches are used to fill the remaining holes in the lattice surface at the transitions. The construction steps are explained in more detail in Section 3.3.

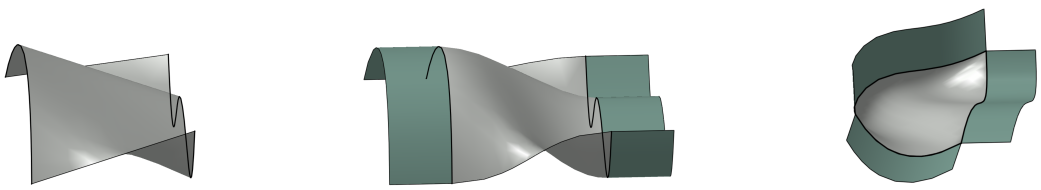

(**a**) (**b**) (**c**)

Figure 1. Sketches of the three types of surface patches that are required for the lattice construction algorithm developed in this work. (**a**) Ruled surface. (**b**) G^1-continuous ruled surface. (**c**) G^1-continuous 3-patch.

3. Lattice Construction Algorithm

The algorithm is summarised in the flowchart (Figure 2). First, the inputs, given by the lattice frame and local shape parameters, are read. Then, the lattice frame is subdivided in order to split the construction task into small, independent, and parallelisable pieces. Afterwards, for each of the latter, the applicability of the general construction method is verified. Otherwise, a suitable special case workaround is considered. In any case, the construction is tested for failures and a fallback in geometric continuity is applied if necessary. A set of surface patches that describes the surface of the solidified lattice structure is given as an output. The algorithm is implemented as a macro in CATIA, but it is not limited to this software. It can be reimplemented in any CAD software that enables the construction of the three types of surfaces defined in Section 2.

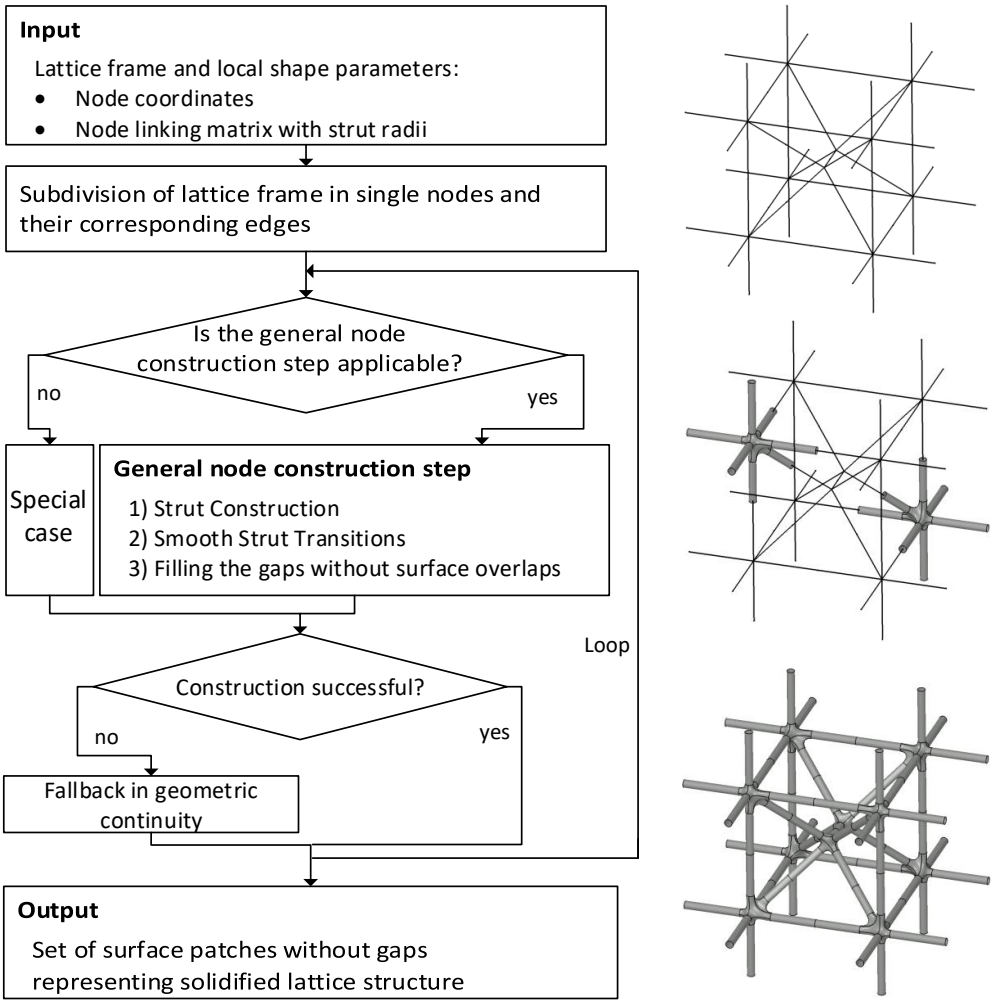

Figure 2. Flowchart of the automated lattice construction algorithm.

3.1. Input and Output

The input to the proposed construction method consists of the lattice frame and of strut radii. For each node, the associated coordinates are required and, for each edge, two radii are to be defined, one per end. Thus, lattice structures with thickness gradients can be constructed. The coordinates as well as the linking and radii information are stored in matrices, which could be generated by any lattice frame design algorithm. In this work, they are assumed to be given. Figure 3 gives an overview of the lattice parameters.

The developed algorithm solidifies the lattice frame by generating a set of surface patches that describes the lattice structures' surface without gaps.

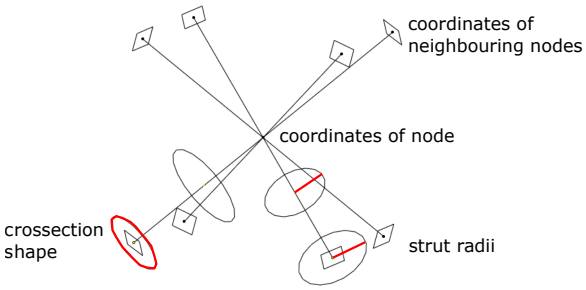

Figure 3. Parameters of the lattice structure.

3.2. Subdivision of the Lattice Structure

The developed method constructs the surface of the lattice structure iteratively. In each step, a smooth transition corresponding to one node of the lattice frame and half of the struts converging to that node are created (Figure 4). Combining the construction of transitions and struts in each step guarantees the availability of the boundary conditions that are required for G^1-continuous transitions. However, the steps are independent of each other and can be parallelised. Furthermore, parameter adjustments, special-case workarounds, and fallback mechanisms can be applied locally in case the general node construction method fails to construct the transition.

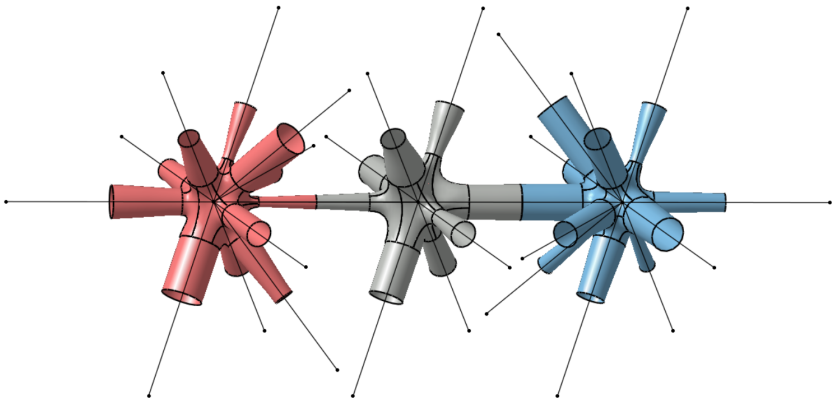

Figure 4. Lattice frame with its respective lattice structure. The colouring of the surface patches shows the subdivision of the construction task in single nodes and halves of their corresponding struts.

3.3. General Node Construction Step

To each node of the lattice frame, the construction algorithm (Figure 5) is applied. Its input is a subset of the original lattice frame that composes only the node itself and nodes that are connected with an edge to this node, denoted as *neighbouring nodes*, as well as the desired strut radii at both ends of these edges. The construction stages are the following:

1. Strut construction
   (a) For each neighbouring node, a point is constructed in the centre of the corresponding edge. In this point and perpendicular to the edge, a plane is defined in that a circle is constructed. The radius of the latter is chosen such that the given radii at the endpoints of the corresponding edge are interpolated linearly. Also perpendicular to the edge, a second plane and a circle within it are constructed (Figure 5a). The intersection point of the second plane with the edge is chosen far enough from the node such that the created circles corresponding to different edges are not intersecting each other. The radii of these circles are given by the input radii of the respective edges. By modifying the radii of the circles or by substituting the circles with other cross-section shapes in this step, the lattice structure is parametrised locally and exactly.

(b) The circles constructed in the previous stage are copied and shifted about a small distance along their respective edges. Each circle and its copy are used as a pair of boundary curves for the definition of ruled surfaces (Figure 5b).

(c) Along the circles, the ruled surfaces constructed in the previous stage are defining tangent planes. Thus, there is a G^1-continuous ruled surface connecting the two original circles for each edge (Figure 5c). By that, the construction of the struts of the final lattice structure is already completed.

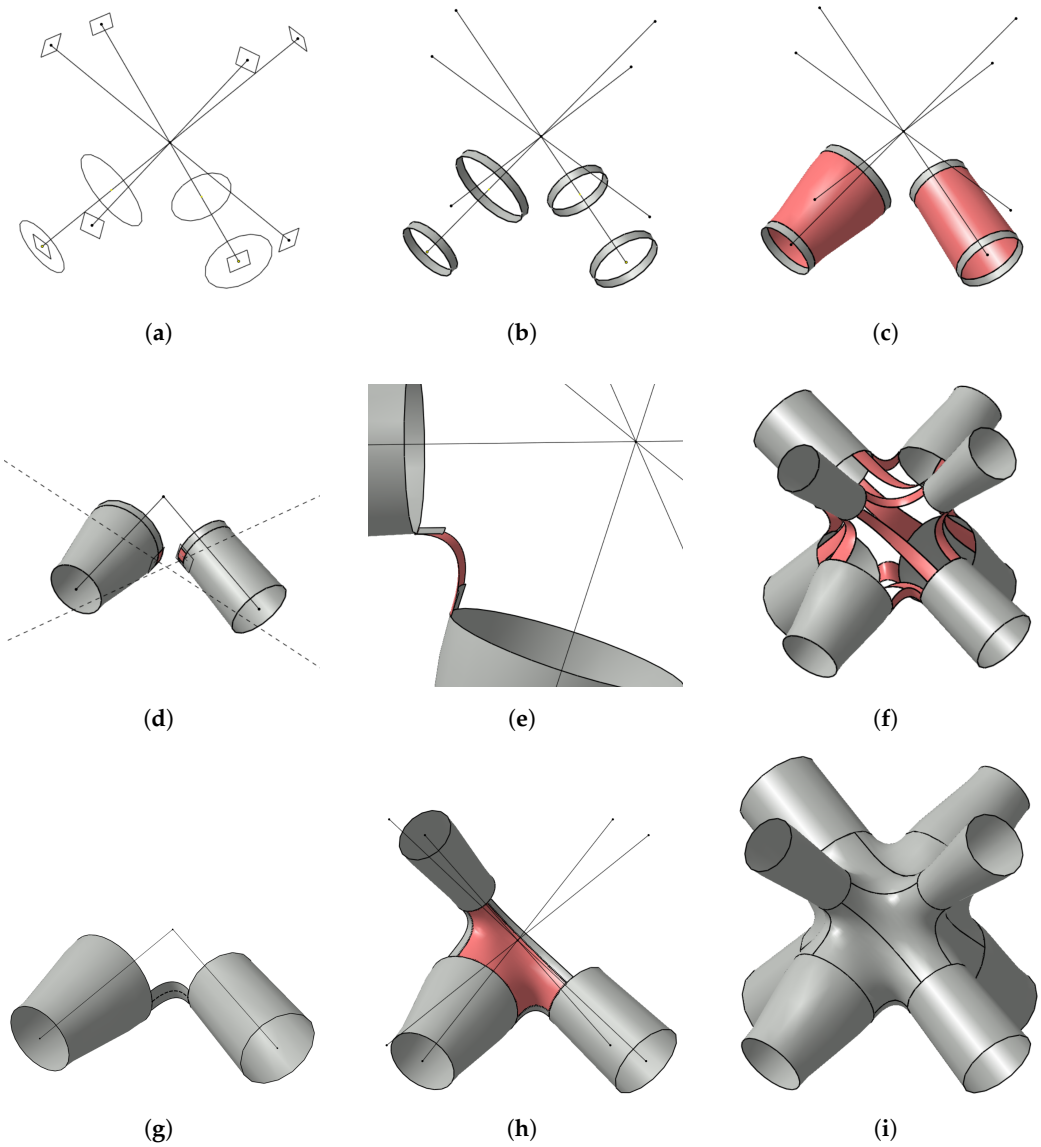

Figure 5. Sketches of the most important stages of the general node construction step. The subfigures (**a**–**i**) represent the sequence of action.

2. Smooth strut transitions

(a) Now, suitable segments of the inner ruled surfaces are cut in order to define boundary conditions for smooth strut transitions. For each pair of struts that shall be connected, the plane spanned by the corresponding edges is intersected with the respective inner planes defined in strut construction step 1a. As a result, the dashed intersection lines (Figure 5d) are obtained. On each of these lines and within the circle, a point is chosen close to the latter. In this point, a plane perpendicular to the intersection line is defined. The inner ruled surface is cut through this plane, leading to the desired small segments (Figure 5d).

(b) In this construction stage, G^1-continuous ruled surfaces are defined that smoothly connect some of the strut segments (Figure 5e). The decision of which segments (Figure 5f) should be connected is taken according to the geometry of the iteratively computed convex hull representation that is determined as follows: Initially, the convex hull of the points corresponding to the neighbouring nodes is computed. If one of these points is in the interior, i.e., the point is not a vertex of the convex hull, it is projected along its corresponding edge on the convex hull's boundary. Then, the convex hull is iteratively recomputed and not simplified until each neighbouring node is represented by one vertex of the convex hull. This representation serves as an abstract model of the desired smooth node and is denoted as *convex hull representation*. Edges of the convex hull are translated into transitions using G^1-continuous ruled surfaces and the triangular faces of the convex hull are translated into G^1-continuous 6-patches filling the regions without gaps that are bounded by struts and their transitions (Figure 6).

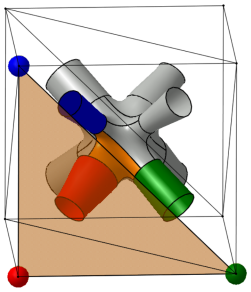

Figure 6. Convex hull representation of a node. A triangular face of the convex hull and the corresponding G^1-continuous 6-patches that is constructed by the lattice algorithm are marked in orange.

3. Filling the gaps without surface overlaps
   (a) In the last construction stage, G^1-continuous 6-patches are created for each face of the convex hull representation. Therefore, boundary curves are selected on the ruled surfaces that were constructed in the previous step. Each of the latter is intersected with the plane spanned by the two edges corresponding to the struts. The result of this intersection is the dashed curve (Figure 5g). Concatenating these curves with segments of the inner circles, constructed in the first strut construction step, the boundary of a 6-patch is defined. The tangent plane along this boundary curve is well-defined by the surface patches that were already constructed. The resulting 6-patch smoothly fills the region between three neighbouring struts (Figure 5h).
   (b) After having created one G^1-continuous 6-patch per face of the convex hull representation and one G^1-continuous ruled surface per neighbouring node, the ruled surfaces constructed in construction step 1b as well as 2b become obsolete for the representation of the lattice structures' surface, because they are overlapping with other patches. Therefore, they can be neglected in the final set of surface patches that serves as an output for each node of the lattice frame (Figure 5i).

3.4. Special-Case Workarounds and Continuity Fallback Mechanism

The automated construction of smooth strut transitions using the general node construction step requires some basic properties of the lattice frame:

1. The neighbouring nodes of each node should not be coplanar or almost coplanar, i.e., more than three neighbouring nodes are required.

2. The edges converging to a node should be distributed equally in space around the node such that in every half-space exists at least one edge.
3. Sharp angles between edges should be avoided.

If the first or the second basic property are not met, the convex hull representation is inappropriate to identify neighbouring struts that can be reasonably connected with smooth strut transitions, as shown in Figure 5f. In these cases, it is likely that the constructed strut transitions lead to self-intersections of the resulting surface. Similarly, if the wireframe has sharp angles, the resulting smooth strut transitions and 6-patches are more likely to intersect each other due to their high curvature. Therefore, nodes that fail to comply with these basic properties are automatically identified by the algorithm and a special-case workaround or a fallback mechanism are applied. The latter are explained in more detail in the following sections.

3.4.1. Workaround for Coplanar and Almost Coplanar Nodes

If there is a plane through the node, such that edges to all neighbouring nodes include small angles to that plane, the special-case workaround for coplanar and almost coplanar nodes is applied. For this node geometry, the occurrence of edges in the convex hull representation is not a suitable measure to detect struts that should be connected by a ruled surface. A more convenient measure is the corresponding edges' polar angle. Ordered according to the value of their polar angle, neighbouring struts are connected with G^1-continuous ruled surfaces. Additionally, surface patches of circular disks are constructed parallel to the plane of coplanarity above and below the node. On the basis of these patches, each strut is connected by a G^1-continuous ruled surface. Finally, the regions between the constructed transitions and struts are filled with G^1-continuous 6-patches. The corresponding construction stages are sketched in Figure 7.

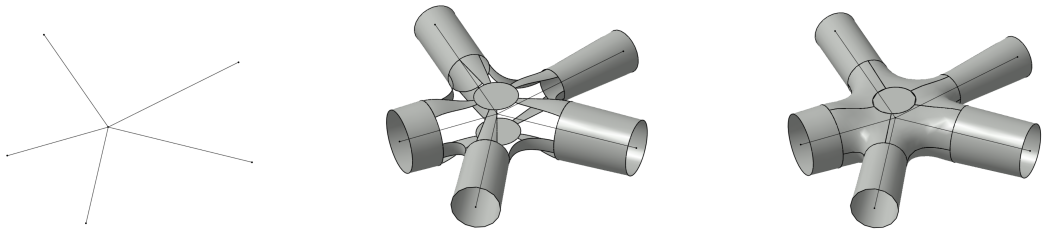

(**a**) (**b**) (**c**)

Figure 7. Construction stages for nodes with coplanar and almost coplanar edges. The subfigures (**a**–**c**) represent the sequence of action.

3.4.2. Workaround for Nodes with Edge-Free Half-Spaces

A node is not in the interior of the convex hull of its neighbouring nodes if the edges are unequally distributed around the node in a way such that edge-free half-spaces exist. Therefore, the convex hull representation fails to identify suitable neighbouring struts. In this case, a makeshift construction point, treated as neighbouring node, is defined in the edge-free half-space such that the node is in the interior of the updated convex hull (Figure 8a). Then, the node is constructed using the general node construction step. Finally, the extra strut, pointing to the makeshift construction point, and parts of the 6-patches next to this strut, are cut off in a small neighbourhood of the strut, as seen in Figure 8b. The resulting hole, bounded by 6-patches, is filled with a G^1-continuous N-patch (Figure 8c).

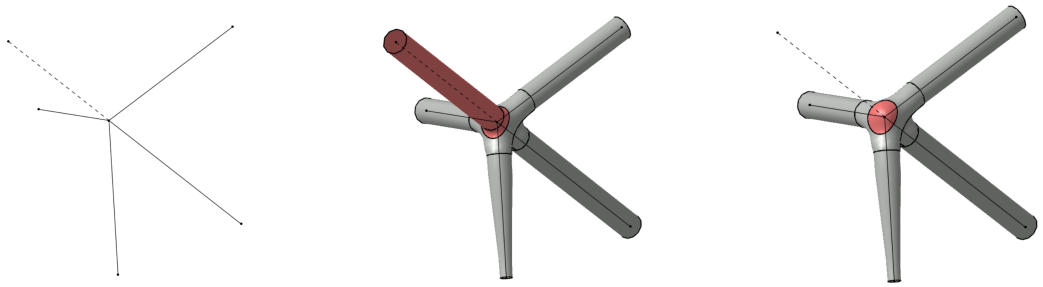

(**a**) (**b**) (**c**)

Figure 8. Construction stages for nodes with edge-free half-spaces. The subfigures (**a**–**c**) represent the sequence of action.

3.4.3. Geometric Continuity Fallback for Sharp Angles and Intricate Input

In the general node construction step, the length of struts converging to the same node is adjusted such that they are not intersecting each other. If two edges enclose a sharp angle, the corresponding struts have to be cut far from the respective node to avoid intersections. But these struts still need to be connected smoothly to other struts. As a result, the constructed smooth transitions with ruled surfaces may intersect each other. To overcome this error, the cross-boundary tangent condition in the definition of strut transitions is dropped. Ruled surfaces are used instead of G^1-continuous ruled surfaces (Figure 9b). Consequently, the resulting node is partly G^0-continuous instead of G^1-continuous.

Even tough the discussed special case workarounds and fallback mechanism of the general node construction step are able to handle various node topologies, the construction of single nodes may still fail or may even be rendered impossible due to intricate input, e.g., regarding the relation of strut radii and length and resulting self-intersections. In order to not interrupt the construction algorithm in this case, a complete fallback mechanism to G^0-continuity is integrated (Figure 9c). A ruled surface is constructed for each edge converging to the node and they are joined by Boolean operations. Due to the parallelised approach, the construction of the respective node can be repeated independently of the other nodes in the lattice frame in a post-processing step if G^1-continuity is required in each node. The repetition can be conducted, for example, with more sensitive special-case recognition parameters or adjusted radii inputs.

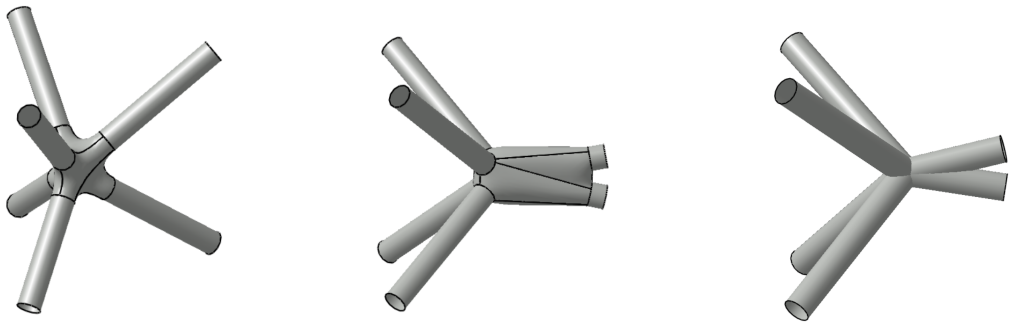

(**a**) (**b**) (**c**)

Figure 9. Different stages of fallback in geometric continuity due to sharp angles and short struts. (**a**) G^1-continuity. (**b**) Partly fallback to G^0-continuity. (**c**) Complete fallback to G^0-continuity.

4. Demonstration, Application, and Discussion

The developed algorithm is demonstrated on the elementary cell of a body-centric cubic lattice structure in three different versions (Figure 10). First, the elementary cell is constructed with constant strut radii and periodic node distribution (Figure 10a). Then, the construction is repeated but with randomly shifted nodes (Figure 10b) and with randomly varied strut radii (Figure 10c).

In Figure 11, a lattice structure composed of eight elementary cells with different unit cell topologies is shown in two versions. First, only the topology is varied (Figure 11a). Then, strut radii and node positions are varied additionally (Figure 11b).

It is seen in these examples that the proposed method is able to construct unit-cell-based lattice structures as well as such with irregular topologies. Furthermore, radii gradients between the ends of a single strut and between struts converging to the same node can be realised and parametrised exactly. As a result, the proposed method is particularly suitable for lightweight design constructions of irregular shapes and radius gradients such as lattice structures derived form topology optimisation results.

Nevertheless, it is not always possible to construct a smooth node. Just as the lattice construction methods in [13,14], the proposed general node construction step shows difficulties with sharp and wide angles between struts because the convex hull-based smooth transition design is not practicable. To overcome this issue, different special-case workarounds and a fallback mechanism in geometric continuity are integrated in the algorithm. Among the nodes shown in Figure 10, there is one node in the top-left corner of Figure 10b, to which the automatic fallback mechanism in geometric continuity is applied. All the other nodes are constructable with the general node construction step. Also in the lattice shown in Figure 11b, the fallback is used twice. However, due to the subdivision of the lattice construction task in node-wise steps, the nodes that are constructed using the fallback mechanism remain accessible for post-processing and their construction can be repeated with different parameters without affecting other parts of the lattice structure.

Furthermore, another advantage of the node-wise subdivision of the construction task is the resulting parallelisability. Therefore, the speed can be increased by orders of magnitude, which is crucial to handle large-scale lattice structures and to integrate it in existing construction software. Requiring, besides basic geometric operations, only the three different patch construction methods described in Section 2 for the generation of surface patches, the developed algorithm can be integrated in any standard CAD software that supports the latter.

The construction time of the 35-node lattice in Figure 11b was recorded. It took five minutes and eight seconds to construct the whole lattice structure even without using the parallelisation on a standard desktop PC. This corresponds to a construction time of 8.8 seconds, per node. Compared to the construction time of approximately one hour per node using the manual scheme in [17], the developed method in this paper is distinctly faster.

The lattice construction algorithm was applied to construct lattice infills for an aircraft component [8]. Pictures of the corresponding additively manufactured component produced using selective laser melting (SLM) can be seen in Figure 12. The position of the lattice infills is chosen in areas where the topology should be strengthened without using solid material. Compared to solid material, the lattice structure is lighter and experiences less thermal deformation during the manufacturing process. The wireframe is designed to enable manufacturing using SLM without additional support structures. The smooth nodes of the lattice reduce stress concentrations. Constructing the lattice infill using surface patches facilitated the construction of smooth interfaces between the infill and the surrounding geometry. In Figure 13, SLM-manufactured lattice cell cubes with topological and radii gradients are depicted.

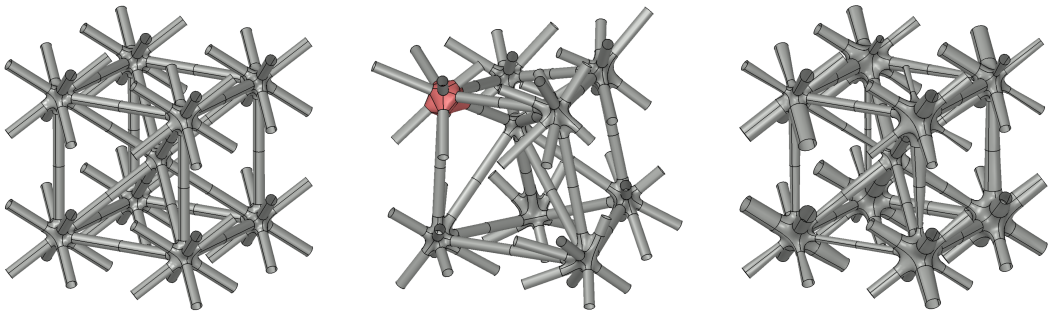

(**a**) (**b**) (**c**)

Figure 10. Lattice construction algorithm applied for a body-centric cubic elementary cell. (**a**) Standard version. (**b**) Randomly shifted nodes. (**c**) Randomly varied radii.

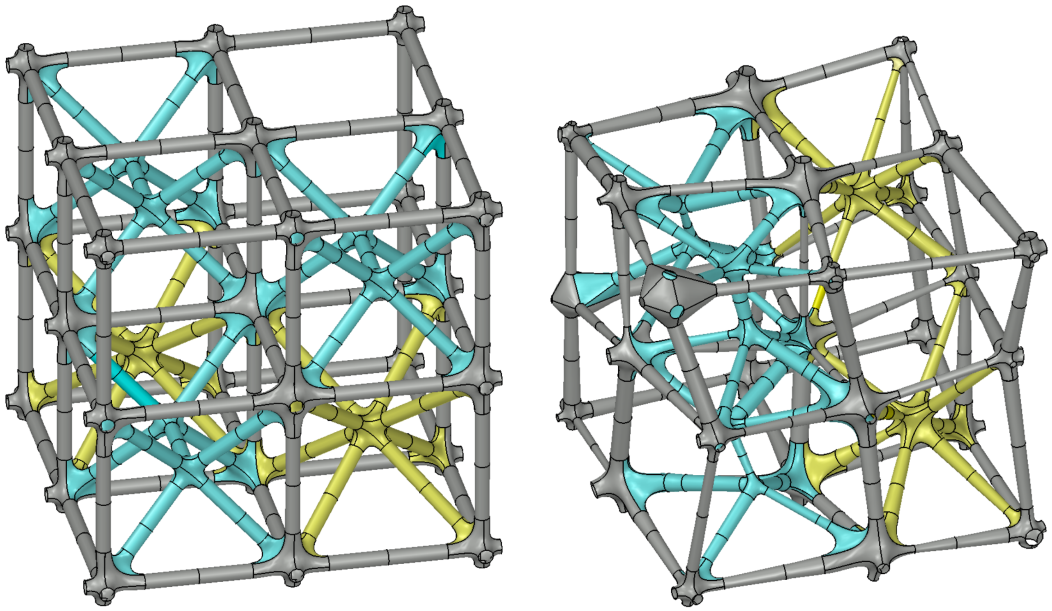

(**a**) (**b**)

Figure 11. Lattice construction algorithm applied for an irregular lattice frame in two configurations. Identical cell topologies are visualised by colour. (**a**) Standard version. (**b**) Randomly shifted nodes and randomly varied radii.

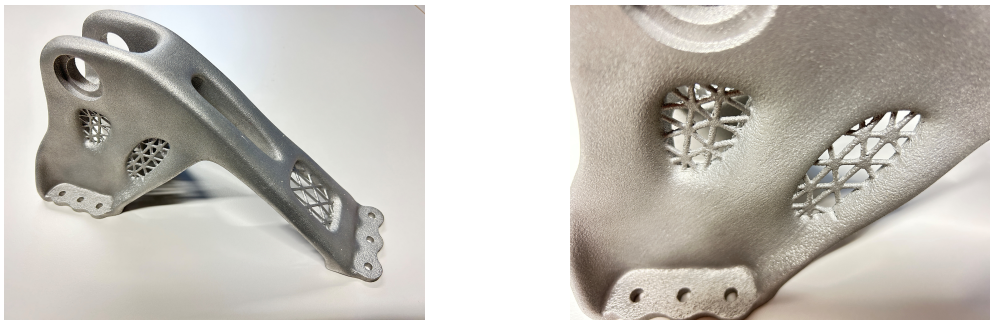

Figure 12. (**Left**): Additively manufactured aircraft component with lattice infills, which are constructed using the discussed method. (**Right**): Zoom in to lattice infill.

Figure 13. Additively manufactured lattice cubes with topology and radii gradients that are constructed using the discussed method.

5. Conclusions

In this work, an automated surface patch-based algorithm is proposed that can smoothly solidify lattice frames with a large variety of topologies. At the same time, local shape parameters, such as strut radii, are exactly and individually modifiable. Specific strut configurations, such as coplanar nodes, nodes with edge-free half spaces, and nodes that contain sharp edges, are limitations to our method, because the general node construction step tends to construct a surface with self-intersections in these cases. For some cases, special-case workarounds successfully manage to nevertheless construct smooth node transitions, while other cases are caught by the fallback to G^0-continuity. However, it is desirable to require as few workarounds and fallbacks as possible.

The usability of the proposed algorithm for wireframe solidifications in engineering contexts is demonstrated by applying it for the construction of lattice infills for an additively manufactured aircraft component. Having an algorithm capable of automatically constructing lattice structures when given topology and strut radii as input parameters, further research could focus on the optimisation of the wireframe topology and shape parameters for different applications and load cases and on the robustness of the method regarding dense lattice structures. For the aircraft component, for instance, different lattice structure designs could be investigated regarding their fail-safe behaviour.

Author Contributions: Conceptualization, L.F. and K.H.; Methodology, L.F.; Software, L.F.; Investigation, L.F.; Writing—original draft, L.F.; Writing—review & editing, K.H.; Supervision, K.H.; Project administration, K.H.; Funding acquisition, K.H. All authors have read and agreed to the published version of the manuscript.

Funding: This research received no external funding.

Institutional Review Board Statement: Not applicable.

Informed Consent Statement: Not applicable.

Conflicts of Interest: The authors declare no conflict of interest.

References

1. Tang, Y.; Dong, G.; Zhao, Y.F. A hybrid geometric modeling method for lattice structures fabricated by additive manufacturing. *Int. J. Adv. Manuf. Technol.* **2019**, *102*, 4011–4030. [CrossRef]
2. Nazir, A.; Abate, K.M.; Kumar, A.; Jeng, J.Y. A state-of-the-art review on types, design, optimization, and additive manufacturing of cellular structures. *Int. J. Adv. Manuf. Technol.* **2019**, *104*, 3489–3510. [CrossRef]
3. Feng, J.; Fu, J.; Lin, Z.; Shang, C.; Li, B. A review of the design methods of complex topology structures for 3D printing. *Vis. Comput. Ind. Biomed. Art* **2018**, *1*, 5. [CrossRef] [PubMed]
4. Mahmoud, D.; Elbestawi, M.A. Lattice Structures and Functionally Graded Materials Applications in Additive Manufacturing of Orthopedic Implants: A Review. *J. Manuf. Mater. Process.* **2017**, *1*, 13. [CrossRef]
5. Vaissier, B.; Pernot, J.P.; Chougrani, L.; Véron, P. Parametric design of graded truss lattice structures for enhanced thermal dissipation. *Comput. Aided Des.* **2019**, *115*, 1–12. [CrossRef]

6. Shinde, M.; Ramirez-Chavez, I.E.; Anderson, D.; Fait, J.; Jarrett, M.; Bhate, D. Towards an Ideal Energy Absorber: Relating Failure Mechanisms and Energy Absorption Metrics in Additively Manufactured AlSi10Mg Cellular Structures under Quasistatic Compression. *J. Manuf. Mater. Process.* **2022**, *6*, 140. [CrossRef]
7. Boschetto, A.; Bottini, L.; Macera, L.; Vatanparast, S. Additive Manufacturing for Lightweighting Satellite Platform. *Appl. Sci.* **2023**, *13*, 2809. [CrossRef]
8. Hoschke, K.; Pfaff, A.; Fleig, L.; Bierdel, M.; Jäcklein, M.; Riedel, W.; Hiermaier, S. A Parametric Mesostructure Approach for Robust Design of Additive Manufacturing Parts. In Proceedings of the Fraunhofer Direct Digital Manufacturing Conference (DDMC), Berlin, Germany, 14–15 March 2018.
9. Ramsaier, M.; Till, M.; Schumacher, A.; Rudolph, S. On a Physics-based Reconstruction Algorithm for Generating Clean Parametric Native CAD-Models from Density-based Topology Optimization Results. In Proceedings of the World Congress of Structural and Multidisciplinary Optimization, Beijing, China, 20–24 May 2019.
10. Maskery, I.; Aremu, A.; Parry, L.; Wildman, R.; Tuck, C.; Ashcroft, I. Effective design and simulation of surface-based lattice structures featuring volume fraction and cell type grading. *Mater. Des.* **2018**, *155*, 220–232. [CrossRef]
11. Savio, G.; Meneghello, R.; Concheri, G. Geometric modeling of lattice structures for additive manufacturing. *Rapid Prototyp. J.* **2018**, *24*, 351–360. [CrossRef]
12. Goel, A.; Anand, S. Design of Functionally Graded Lattice Structures using B-splines for Additive Manufacturing. *Procedia Manuf.* **2019**, *34*, 655–665. [CrossRef]
13. Mattingly, W.A.; Chariker, J.H.; Paris, R.; Chang, D.J.; Pani, J.R. 3D modeling of branching structures for anatomical instruction. *J. Vis. Lang. Comput.* **2015**, *29*, 54–62. [CrossRef] [PubMed]
14. Srinivasan, V.; Mandal, E.; Akleman, E. Solidifying Wireframes. In Proceedings of the 2004 Bridges Conference on Mathematical Connections in Art, Music, and Science, 2005. Available online: http://archive.bridgesmathart.org/2005/bridges2005-203.html (accessed on 7 September 2023).
15. Al-Ketan, O.; Lee, D.W.; Rowshan, R.; Abu Al-Rub, R.K. Functionally graded and multi-morphology sheet TPMS lattices: Design, manufacturing, and mechanical properties. *J. Mech. Behav. Biomed. Mater.* **2020**, *102*, 103520. [CrossRef] [PubMed]
16. Hu, C.; Lin, H. Heterogeneous porous scaffold generation using trivariate B-spline solids and triply periodic minimal surfaces. *Graph. Model.* **2021**, *115*, 101105. [CrossRef]
17. Hassani, V.; Khabazi, Z.; Raspall, F.; Banon, C.; Rosen, D. Form-Finding and Structural Shape Optimization of the Metal 3DPrinted Multi-Branch Node with Complex Geometry. *Comput. Aided Des. Appl.* **2019**, *17*, 205–225. [CrossRef]
18. Campbell, R.J.; Flynn, P.J. A survey of free-form object representation and recognition techniques. *Comput. Vis. Image Underst.* **2001**, *81*, 166–210.
19. Gallier, J. *Geometric Methods and Applications: For Computer Science and Engineering*; Springer Science & Business Media: New York, NY, USA, 2001; Volume 38.
20. Farin, G. *Curves and Surfaces for CAGD: A Practical Guide*; Morgan Kaufmann: Burlington, MA, USA, 2002.
21. Schaaf, J.; Ravani, B. Geometric continuity of ruled surfaces. *Comput. Aided Geom. Des.* **1998**, *15*, 289–310. . [CrossRef]
22. Gregory, J.A.; Zhou, J. Filling polygonal holes with bicubic patches. *Comput. Aided Geom. Des.* **1994**, *11*, 391–410. [CrossRef]
23. Chui, C.K.; Lai, M.J. Filling polygonal holes using C1 cubic triangular spline patches. *Comput. Aided Geom. Des.* **2000**, *17*, 297–307. [CrossRef]
24. Piegl, L.A.; Tiller, W. Filling n-sided regions with NURBS patches. *Vis. Comput.* **1999**, *15*, 77–89. [CrossRef]